

Synthesis and Nonlinear Optical Properties of Three-Dimensional Phosphonium Ion Chromophores**

Christoph Lambert,* Elmar Schmäzlin, Klaus Meerholz, and Christoph Bräuchle

Abstract: Here we describe the synthesis and the linear and nonlinear optical properties of three dibutylaminoazobenzene phosphonium salt chromophores: a one-dimensional system with one azobenzene subchromophore and two three-dimensional systems, one with C_3 symmetry (three subchromophores) and one with approximate T symmetry (four subchromophores). Experimental investigations (UV/Vis spectroscopy and hyper-Rayleigh scattering), theoretical calculations (exciton coupling theory and tensor transformations), as well as computational calculations (PM3/time-dependent Hartree–Fock) show that, while the linear optical properties of the 3D compounds behave additively, the first-order hyperpolarisability β is distinctly enhanced in the 3D compounds relative to the 1D derivative.

Keywords: azo compounds • nonlinear optics • phosphorus • semi-empirical calculations

Introduction

Organic second- and third-order nonlinear optical (NLO) materials are of great importance in future optoelectronic technology.^[1] Among others, the effects mostly studied are second- and third-harmonic generation (SHG and THG), linear and nonlinear electrooptic effects (Pockels and Kerr effects), and organic photorefractive. In the case of one-dimensional (1D) push/pull substituted chromophores for second-order nonlinear optical applications such as SHG or the Pockels effect, the underlying relations between molecular and electronic structure and microscopic optical nonlinearity, as well as the macroscopic nonlinearity of the crystalline or polymeric bulk material, are now reasonably well understood. Semiquantitative descriptions such as bond length alternation^[2] or two-level approximation^[3] [see Eq. (9)] are widely used to design and tune new NLO chromophores. A major drawback of conventional chromophores is the so-called nonlinearity/transparency trade-off: for a given type of π chromophore the hyperpolarisability increase is accompanied by a red shift of the absorption maximum (decreasing blue transparency),^[4] which can cause

reabsorption of the second-harmonic light. Alternative chromophores that have recently been synthesised and investigated^[5] include zwitterions,^[6] intramolecular charge-transfer (CT) complexes,^[7] molecules with C_{2v} symmetry (which possess CT moments orthogonally polarised to the dipolar axis and consequently octopolar contributions to the first-order hyperpolarisability),^[8] and molecules with D_{3h} symmetry (purely octopolar β tensor).^[9, 10] The major reason for the investigation of these chromophores is to circumvent or at least to improve the nonlinearity/transparency trade-off. Although purely octopolar molecules show no ground-state dipole moment and thus cannot be oriented (e.g., poled) by conventional techniques in polymer matrices, they are promising candidates for crystalline materials, as the lack of a dipole moment should favour a noncentrosymmetric arrangement of the chromophores in the crystal lattice,^[9] a prerequisite for observing second-order nonlinear optical effects in the solid state.

While one-dimensional molecules with a charge transfer polarised along the molecular z axis (e.g., 4,4'-dimethylaminonitrostilbene, DANS) have a β tensor dominated by one element, β_{zzz} , an additional off-diagonal tensor element, β_{zyy} , becomes important in C_{2v} symmetric chromophores such as 3,5-dinitroaniline. Substituted binaphthol derivatives with C_2 symmetry^[11] and cobalt complexes of Schiff bases^[12] were also investigated and compared to their subchromophore counterparts; the nonzero tensor elements in these cases also are β_{zzz} and β_{zyy} . Finally, in D_{3h} -symmetric molecules (e.g., triaminotrinitrobenzene), there is a degenerate excited CT state with nonvanishing tensor elements $\beta_{yyy} = -\beta_{xxy}$.^[10] In contrast, molecules with three-dimensional CT states such as T -

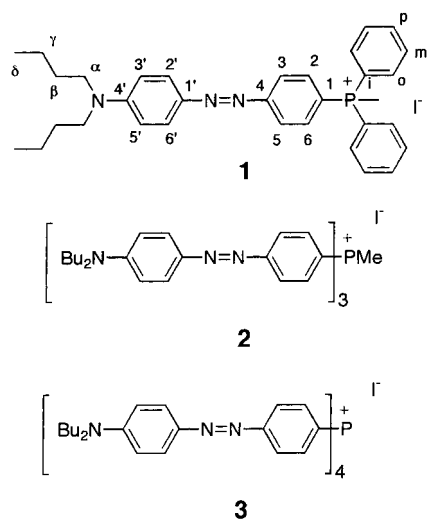
[*] Dr. C. Lambert

Institut für Organische Chemie der Universität
Universitätsstr. 31, D-93040 Regensburg (Germany)
Fax.: (+ 49) 0941-943 4984

Dipl.-Chem. E. Schmäzlin, Dr. K. Meerholz, Prof. Dr. C. Bräuchle
Institut für Physikalische Chemie der Ludwig-Maximilians-Universität
München
Sophienstr. 11, D-80333 München (Germany)

symmetric chromophores (only β_{xyz} is nonzero) with a triply degenerate excited state have attracted little attention. To our knowledge, only one series of tetrasubstituted tin compounds has been investigated so far.^[13]

We have synthesised a 4,4'-substituted azobenzene molecule with a conventional dialkylamino donor functionality and an ionic triorganophosphonium acceptor group as the 1D reference chromophore **1**. As we have shown recently for



ammonium/borate zwitterions, ionic groups like triorganophosphonium are very efficient electron acceptors and lead to highly blue-transparent NLO chromophores.^[6b] Thus, it was obvious to use a charged phosphonium centre to connect one, three and four azobenzene subchromophores in order to construct the 1D reference system, a 3D chromophore with three side wings and C_3 symmetry **2**, and a 3D chromophore with four side wings and D_2 (approximate T) symmetry **3**. Using theoretical, computational (PM3/time-dependent Hartree–Fock, TDHF) and experimental (hyper-Rayleigh scattering, HRS) methods, we address the linear and nonlinear optical relations between the two 3D and the 1D chromophores. We show that, while the linear properties construct additively, the nonlinear properties are substantially enhanced in the 3D cases.

Abstract in German: Wir beschreiben in dieser Arbeit die linearen und nichtlinearen optischen Eigenschaften dreier Dibutylaminoazobenzolphosphonium-Salz-Chromophore:

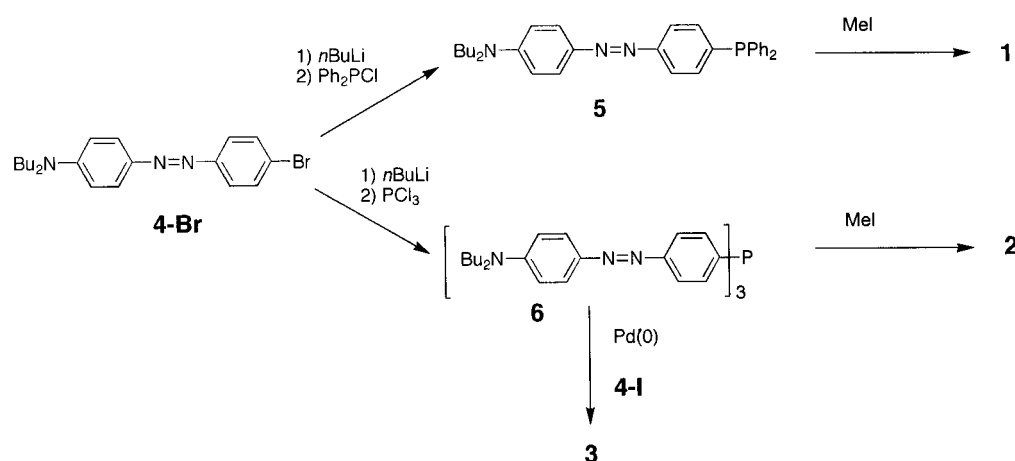
Ein eindimensionales System mit einem Azobenzol-Subchromophor und zwei dreidimensionale Systeme, eines davon mit C_3 -Symmetrie (drei Subchromophore) und eines, das annähernd T -Symmetrie besitzt (vier Subchromophore). Experimentelle Untersuchungen (UV/Vis-Spektroskopie und Hyper-Rayleigh-Streuung), theoretische Berechnungen (Theorie der gekoppelten Exzitonen und Tensor-Transformationen) sowie Computerberechnungen (PM3/time-dependent Hartree–Fock) zeigen, daß, obwohl sich die linearen optischen Eigenschaften der 3D-Chromophore additiv verhalten, die Hyperpolarisierbarkeit erster Ordnung der 3D-Verbindungen deutlich gegenüber dem 1D-Referenzchromophor verstärkt ist.

Results

A. Synthesis: Although in terms of transparency azobenzenes are not promising candidates, a substituted azobenzene derivative was chosen as a model chromophore because it combines several advantages: it is easily accessible and reasonably stable to light and heat,^[14] and chromophores composed of azobenzenes are unlikely to fluoresce at room temperature^[15] (this might otherwise interfere with the HRS signal by two- or three-photon-induced fluorescence; see Section C). Tetraorganophosphonium ions as anion-stabilising (electron-withdrawing) groups have long been known and are extensively used in synthetic organic chemistry in the form of phosphonium (Wittig) ylides.^[16] Although arylphosphane oxides and arylphosphonates have frequently been used as acceptor groups in push/pull substituted π -electron systems for NLO applications,^[17] we are aware of only one study concerning phosphonium ions in this respect.^[6a] The synthesis of compounds **1–3** is outlined in Scheme 1. Reaction of the lithiated azobenzene derivative with Ph_2PCl or PCl_3 , respectively, leads to **5** and **6**, which were subsequently quaternised with methyl iodide. Compound **3** was synthesised by a palladium(0)-catalysed reaction^[18] from **5** with the iodoazobenzene derivative **4-I**. All salts were purified by column chromatography and are hygroscopic crystalline solids (**1**) or low-melting glasses (**2, 3**).

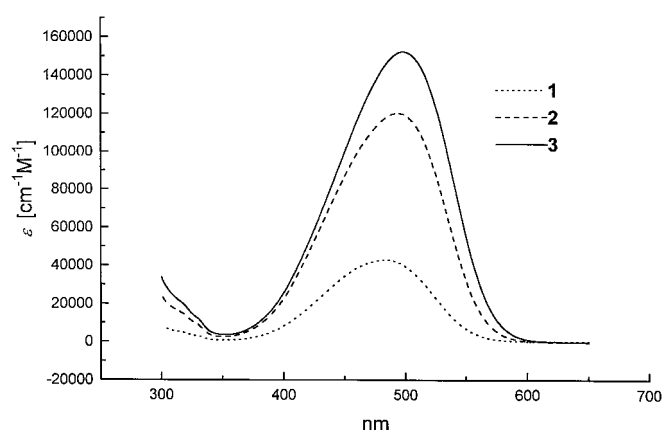
B. Linear optical properties: The UV/Vis spectral data of compounds **1–3** were recorded in MeCN and CHCl_3 and are listed in Table 1 and shown in Figure 1. There is a marked red shift of 461 (611) cm^{-1} and 666 (833) cm^{-1} between **1** and **2**, and **1** and **3** in MeCN (CHCl_3), which can be explained by exciton coupling theory (see Section E). Numerical integration of the absorption band shape yields the oscillator strengths $f = 4.319 \times 10^{-9} \int \epsilon(\tilde{\nu}) d\tilde{\nu}$ in a 1/2.92/3.64 ratio for **1–3**, as expected for noninteracting chromophores (1:3:4) (see Section E). All derivatives show a small negative solvatochromism between CHCl_3 and MeCN solutions: -329 cm^{-1} (**1**), -479 cm^{-1} (**2**), and -496 cm^{-1} (**3**).

C. Nonlinear optical properties: The hyperpolarisability β of **1–3** was measured by hyper-Rayleigh scattering in MeCN,^[19] since the conventional EFISH method is not applicable to charged molecules. The 1300 nm output of an optical parametric power oscillator (OPPO) system^[20] was used to circumvent problems with reabsorption at the second harmonic (650 nm), for which all derivatives are completely transparent. In addition, two-photon-induced fluorescence will not contribute to the SHG signal at this wavelength;^[21] this interfering process, as well as three-photon-induced fluorescence, is unlikely for **1–3** as they do not fluoresce at room temperature, as expected for azo dyes.^[15] The unpolarised HRS signal^[22] was measured against *p*-dimethylaminocinnamaldehyde ($\beta_{zzz} = 66 \times 10^{-30}$ esu at 1300 nm in MeCN; $\lambda_{\text{max}} = 379$ nm) as an external standard, which in turn was measured against *p*-nitroaniline ($\beta_{zzz} = 29.2 \times 10^{-30}$ esu at 1064 nm in MeCN;^[24] $\lambda_{\text{max}} = 366$ nm). In the external reference method, $I(2\omega)$ was measured for a series of solutions of the molecule under investigation with varying sample con-

Scheme 1. Synthesis of **1**, **2** and **3**.Table 1. UV/Vis spectral data of **1–3**.^[a]

	MeCN				CHCl ₃
	$\tilde{\nu}_{\max}$ [cm ⁻¹] (λ_{\max} [nm])	$\epsilon \times 10^3$ [M ⁻¹ cm ⁻¹]	f	f_{rel}	$\tilde{\nu}_{\max}$ [cm ⁻¹] (λ_{\max} [nm])
1	20717 (483)	34.1	0.845	1.000	20388 (491)
2	20256 (494)	120.8	2.465	2.917	19777 (506)
3	20051 (499)	152.7	3.076	3.640	19555 (511)

[a] ϵ : extinction coefficient; f : oscillator strength; f_{rel} : relative oscillator strength.

Figure 1. UV spectra of **1**, **2** and **3** in MeCN.

centration, and then the measurement was repeated in the same solvent under identical experimental conditions for a reference solute whose symmetry and β value are known. A plot of $I(2\omega)/I(\omega)^2$ versus the number density for both sample and reference solute was made. The ratio of the two slopes is related to the ratio of the solute and reference $\langle\beta_{\text{HRS}}^2\rangle$ values, where $\langle\beta_{\text{HRS}}^2\rangle$ is the orientational average of the square of the first hyperpolarisability of the solvated molecule. Finally, specific components of the β tensor of the sample may be determined from $\langle\beta_{\text{HRS}}^2\rangle_{\text{sample}}/\langle\beta_{\text{HRS}}^2\rangle_{\text{reference}}$ if the sample solute symmetry is known. The $\beta^{\text{B}*}$ convention of Willets et al.^[25] was adopted throughout this paper. The detailed experimental setup and data evaluation procedure can be found in ref. [20]. Compounds **1–3** were investigated in MeCN to avoid problems with aggregation. Indeed, the HRS intensity versus number density plot does not show the significant deviation

from linearity that would be expected for concentration-dependent aggregation. Data evaluation leads to averaged isotropic $\langle\beta_{\text{HRS}}^2\rangle$ values at 1300 nm (see Table 2), which were converted to static values by using the dispersion term of Equation (7) (see Section E) with the assumption that $\omega_{0n'} = \omega_{0n} = \omega_{\text{CT}}$, where ω_{CT} denotes the experimentally determined charge-transfer frequency. In the following, we refer to static β values.

The sign of β cannot be determined by HRS. The negative solvatochromism of **1** suggests a negative dipole moment difference between ground and excited state (see Section D) and hence a negative β_{zzz} .^[6b] Depending on the molecular symmetry, only some of the ten different β tensor elements (assuming Kleinman symmetry) are nonvanishing and contribute to $\langle\beta_{\text{HRS}}^2\rangle$. For the 1D chromophore **1**, β_{zzz} dominates; all other tensor elements are smaller than 5% of β_{zzz} or zero (see Section D). For a composite molecule with C_3 symmetry composed of 1D chromophores, $-\beta_{xyy} = \beta_{yyy}$, β_{zzz} , $-\beta_{xyy} = \beta_{xxx}$, and $\beta_{yyz} = \beta_{zxx}$ are nonvanishing. For a molecule with D_2 or T symmetry, only β_{xyz} is nonzero. Thus, for 1D molecules and 3D molecules with C_3 and $D_2(T)$ symmetry, $\langle\beta_{\text{HRS}}^2\rangle$ is given by Equations (1)–(3).^[10f, 13b, 26, 27]

$$1\text{D} \quad C_1 \quad \langle\beta_{\text{HRS}}^2\rangle = \frac{6}{35}\beta_{zzz}^2 \quad (1)$$

$$3\text{D} \quad C_3 \quad \langle\beta_{\text{HRS}}^2\rangle = \frac{8}{21}(\beta_{xxx}^2 + \beta_{xyy}^2) + \frac{6}{35}\beta_{zzz}^2 + \frac{92}{105}\beta_{xxz}^2 + \frac{32}{105}\beta_{xxz}\beta_{zzz} \quad (2)$$

$$3\text{D} \quad D_2 \text{ or } T \quad \langle\beta_{\text{HRS}}^2\rangle = \frac{4}{7}\beta_{xyz}^2 \quad (3)$$

The experimentally determined $\langle\beta_{\text{HRS}}^2\rangle^{1/2}$, the corresponding static β_{ijk} values and the modulus $\|\beta^0\| = \sqrt{\sum_{ijk} \beta_{ijk}^2}$, which is commonly employed to compare β values of molecules with octopolar contributions,^[9, 10b] for **1–3** are given in Table 2. It is not possible to deduce β_{xyy} , β_{xxz} and β_{zzz} of **2** from the measured $\langle\beta_{\text{HRS}}^2\rangle$ value ($-\beta_{xyy} = \beta_{xxx} = 0$ due to the 1D nature of the subchromophore^[28]); therefore, we used the theoretical ratio (see Section E) of $\beta_{xyy}:\beta_{xxz}:\beta_{zzz}$ to estimate these values.

D. Computational calculations: Compounds **1–3** (*N*-butyl groups were replaced by *N*-methyl for simplicity) were optimised with the PM3 Hamiltonian implemented in the MOPAC 93 program package.^[29] Although it is well known that (*E*)-azobenzene dyes may be twisted,^[30] the 1D sub-

Table 2. Static hyperpolarisability in 10^{-30} esu of **1–3**. Left part: absolute experimental values at 1300 nm and absolute static values; right part: relative values obtained by dividing the PM3 values by 53.3×10^{-30} esu and the experimental values by 61.6×10^{-30} esu. The error has been estimated to be $\pm 15\%$. The conversion factor for β to SI units: 1×10^{-30} esu = 3.713×10^{-51} C m³ V⁻².

1 , C_1	$\langle \beta_{\text{HRS}}^2 \rangle^{1/2}$ at 1300 nm	$\langle \beta_{\text{HRS}}^0 \rangle^{1/2}$	β_{zzz}^0 [a,d]	$ \beta^0 $	$\langle \beta_{\text{HRS}}^0 \rangle^{1/2\text{rel}}$	β_{zzz}^{rel}	$ \beta^0 ^{\text{rel}}$					
	theor.: exciton cpl. = tensor add. PM3/TDHF HRS		22.1 65.9	53.3 61.6	53.3 61.6	0.414 0.414	1 1	1 1				
2 , C_3			β_{zzz}^0 [a]	β_{xyy}^0 [a]	β_{xxz}^0 [a]	β_{zzz}^{rel}	β_{xyy}^{rel}	β_{xxz}^{rel}				
	theor.: exciton cpl. = tensor add.					0.546	0.053	0.675	0.366	1.62		
	PM3/TDHF		28.9	0.5	39.5	16.4	88.7	0.542	0.009	0.741	0.308	1.66
	HRS	123	44.4	4.3 ^[b]	54.9 ^[b]	29.6 ^[b]	132 ^[b]	0.721	0.070 ^[b]	0.897 ^[b]	0.487 ^[b]	2.16 ^[b]
3 , D_2			β_{xyz}^0 [a]			β_{xyz}^{rel}						
	theor.: tensor add. theor. (T): ^[c] exciton cpl. = tensor add.					0.569 0.582	0.752 0.770	1.84 1.89				
	PM3/TDHF		29.4	38.9	95.3	0.552	0.730	1.79				
	HRS	162	56.7	74.9	184	0.921	1.21	2.98				

[a] All β_{ijk} tensor elements are negative. [b] β_{zzz} , β_{xyy} and β_{xxz} have been calculated from $\langle \beta_{\text{HRS}}^2 \rangle^{1/2}$ by means of the theoretical ratio of 0.053:0.675:0.366. [c] Ideal T symmetry was assumed. [d] All other tensor elements are smaller than 5% or zero.

chromophores in **1–3** were restricted to C_s symmetry to simplify the tensorial analysis. Compounds **2** and **3** were then optimised in C_3 and D_2 symmetry, respectively (see Figure 2). To obtain approximate excited-state properties, we performed CI calculations within a given orbital window. The number of occupied and empty orbitals was chosen to include all orbitals

in a given active space of -10.000 to -3.000 eV. This results in a CI(5,1) for **1**, CI(6,3) for **2** and CI(8,4) for **3**, where X in CI(X , Y) denotes the total number of spatial orbitals, and Y the number of doubly occupied orbitals. The maximum number of energy selected microstates is limited to 121 by the MOPAC program. In Table 3, some ground- and excited-

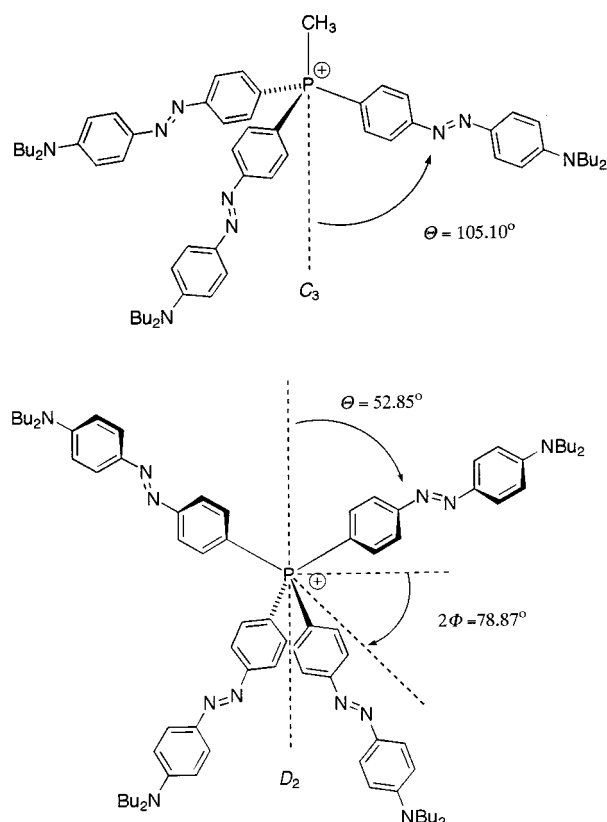


Figure 2. PM3 optimised geometries of **2** and **3**.

Table 3. MOPAC PM3-CI calculated ground- and excited-state properties of **1–3**.^[a]

	μ_0 [D]	μ_a [D]	$\tilde{\nu}_{\text{max}}$ [cm ⁻¹] (λ_{max} [nm])	f
1 CI(5,1)	10.2	-21.8	29988 (334) (A)	0.431
1 CI(8,4)		-14.8	28197 (355) (A)	0.566
2 CI(6,3)	3.0		30544 (327) (E)	1.305
3 CI(8,4)	0.0		30996 (323) (A)	0.069
			32012 (312) (B1)	0.692
			32036 (312) (B2)	0.809
			32036 (312) (B3)	0.427
		32665 (306) (A)	0.000	

[a] μ_0 : ground-state dipole moment; μ_a : excited-state dipole moment; f : oscillator strength.

state properties of **1–3** are given. We emphasise that the limited CI used in our calculations and the neglect of solvent influences will certainly not yield quantitative results, but will give qualitative insight into the electronic nature of the compounds.

The direction of the large ground-state dipole moment (10.2 D) of **1** is reversed in the first excited singlet state (-21.8 D). The magnitude of μ_a is probably overemphasised, since a somewhat larger CI(8,4) calculation gives a smaller μ_a of -14.8 D. The calculation nevertheless confirms a large negative $\Delta\mu = \mu_a - \mu_g$ dipole moment difference upon excitation;^[31] this indicates a significant negative β_{zzz} from the two-level approximation [see Eq. (9)]. Figure 3 illustrates the difference in the Coulson charges between the S_1 and S_0 states of **1**.

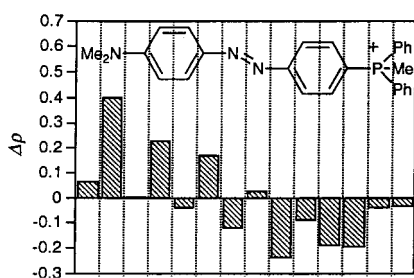


Figure 3. Difference of Coulson charges $\Delta\rho$ between S_0 and S_1 of compound **1**. A positive charge difference denotes loss of electron density upon excitation.

As expected for symmetry reasons, **2** has a doubly degenerate excited E state and one higher lying A state, whereas **3** has a practically triply degenerate excited state and one higher lying A state. Because **3** has D_2 symmetry, the three excited states belong to the irreducible representations B_1 , B_2 , and B_3 , but since **3** approximates T symmetry, these three states are almost degenerate.

The transition energies are similar for all compounds but are distinctly higher than the experimental values. Inclusion of solvent effects (e.g., by an SCRF method^[32]) will not improve the result, as the experiments indicate a negative solvatochromic shift and simulation of the solvent thus should lead to even higher excitation energies. A more detailed comparison of excited-state properties of compounds **1–3** is not justified, because truncated CI expansions are not size-consistent. For this reason, the static first-order hyperpolarisability tensor β_{ijk} was calculated by the time-dependent Hartree–Fock (TDHF) method^[33] and not, as is often done, by a sum-over-states (SOS) approach based on CI expansions.^[34, 35] The results for the respective nonzero β tensor elements of **1–3** are given in Table 2. As suggested by the negative solvatochromism, all β_{ijk} values are negative.

E. Theoretical calculations: exciton coupling theory: Provided that subchromophores interact only weakly in their ground state, exciton coupling theory^[38] can be used to explain band (Davydov) splitting or band shifts of chromophore assemblies due to dipole coupling of subchromophores. In our case, the assumption of weak coupling is justified by a PM3 calculation^[39] which estimates an interaction energy of only 0.28 kJ mol^{-1} per chromophore pair. In the following, we will use this approach to explain the linear and nonlinear optical properties of **1–3**. Calculated eigenstate energies, eigenfunctions and transition moments are used to calculate β by using the SOS expansion [Eq. (7)].

The formalisms of molecular orbital theory were employed, although the physical basis of exciton coupling theory is different. Only a brief description is given here; the basic formalism can be found in ref. [38c]. The reference chromophore p has ground- and excited-state wave functions $\phi_0^{(p)}$ and $\phi_a^{(p)}$, respectively, with associated energies E_0 and E_a . The ground-state wave function of a composite chromophore is given by $\psi_0 = \prod_{p=1}^m \phi_0^{(p)}$ with energy $E_0 = 0$ where $\phi_0^{(p)}$ are orthonormal ground-state wave functions of subchromophore $p, q = 1 - m$. The excited-state wave function is represented by

the linear combination $\psi_a = \sum_{q=1}^m (c_q \prod_{p \neq q=1}^m \phi_0^{(p)} \phi_a^{(q)})$. The eigenvalue problem $\hat{H}\psi_a = E\psi_a$ with $\hat{H} = \sum_{p=1}^m \hat{H}_p \sum_{p \neq q=1}^m \sum_{p=1}^m \hat{H}_{pq}$ has to be solved, where \hat{H}_{pq} for $p \neq q$ is replaced by the point-dipole point-dipole approximation potential [Eq. (4)].

$$V_{pq} = \mu_{0a}^{(p)} \mu_{0a}^{(q)} R_{pq}^{-3} \{ \mathbf{e}_p \cdot \mathbf{e}_q - 3(\mathbf{e}_p \cdot \mathbf{e}_{pq})(\mathbf{e}_q \cdot \mathbf{e}_{pq}) \} \quad (4)$$

In this approximation, $\mu_{0a}^{(p)}$ and $\mu_{0a}^{(q)}$ are the transition moments at molecule p and q , respectively, R_{pq} is the distance between the transition moments, and \mathbf{e}_p , \mathbf{e}_q , and \mathbf{e}_{pq} are the unit vectors of $\mu_{0a}^{(p)}$, $\mu_{0a}^{(q)}$ and R_{pq} . If idealised T symmetry is assumed for **3**, $V_{pq} = V_{12}$ for all combinations of p and q ; then, the secular equations for **2** and **3** are given by Equations (5) and (6), respectively.

$$\begin{vmatrix} E_a - E & V_{12} & V_{12} \\ V_{12} & E_a - E & V_{12} \\ V_{12} & V_{12} & E_a - E \end{vmatrix} = 0 \quad (5)$$

$$\begin{vmatrix} E_a - E & V_{12} & V_{12} & V_{12} \\ V_{12} & E_a - E & V_{12} & V_{12} \\ V_{12} & V_{12} & E_a - E & V_{12} \\ V_{12} & V_{12} & V_{12} & E_a - E \end{vmatrix} = 0 \quad (6)$$

From these equations the following eigenvalues are obtained: $E = E_a + 2V_{12}$ and $2 \times E = E_a - V_{12}$ for **2**, and $E = E_a + 3V_{12}$ and $3 \times E = E_a - V_{12}$ for **3**. The eigenfunctions are given in the Appendix. As expected for symmetry reasons and in agreement with the computational CI calculations, **2** has a doubly degenerate E excited state, and **3** has a triply degenerate T excited state (see Figure 4).

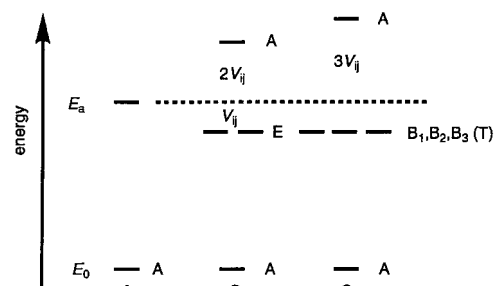


Figure 4. Qualitative energy level diagram of **1**, **2** and **3** from exciton coupling theory.

Using the PM3 optimised geometry for **2** and ideal T symmetry for **3** with a N–P distance of 12.36 \AA gives $R_{12} = 10.33 \text{ \AA}$ for **2** and 10.11 \AA for **3**. The transition moments μ_{0a} in Equation (4) can be calculated from the oscillator strength $f = 4.702 \times 10^{-7} \tilde{\nu} \mu_{0a}^2$ (see Table 1). Evaluation of Equation (4) for **2** and for **3** yields $V_{12} = 673$ and 704 cm^{-1} , respectively (see Figure 4). This is in good agreement with the experimentally observed shift between **1** and **2** (461 cm^{-1}), and **1** and **3** (666 cm^{-1}) in MeCN.

With the above evaluated excited-state wave functions ψ_n and with $\mu_{nr} = \langle \psi_n | \hat{\mu} | \psi_r \rangle$, where $\hat{\mu} = \sum_{p=1}^m \hat{\mu}^{(p)}$ and $\Delta\mu^{(p)} = \mu_{aa}^{(p)} - \mu_{00}^{(p)}$ (since the charge centroid definition has been used,

$\mu_{00}=0$ and thus $\Delta\mu=\mu_{aa}$ ^[40]), one obtains the transition moments between ground and excited states as well as between excited states n and n' of **2** and **3**. These transition moments can be expressed relative to the transition moment μ between the ground and excited state as well as the dipole moment difference $\Delta\mu=\mu_{aa}-\mu_{00}$ of ground and excited state of the 1D subchromophore **1** (the transition moments necessary for the evaluation of β from the SOS expression [Eq. (7)] are given in the Appendix).

These transition moments were used to calculate the β tensor elements from the SOS expression [Eq. (7)].^[40] In this equation, μ_{0n} and $\mu_{n'n}$ denote the transition moments from the ground state to the excited state n and between excited states n and n' , respectively. ω_{0n} are the excitation frequencies and ω denotes the incident radiation frequency. If we assume negligible interchromophoric interaction in the excited state, then $\omega_{01}=\omega_{02}=\omega_{03}$ for **2** and $=\omega_{04}$ for **3**, and Equation (7) reduces to a simple five-level approximation for **3**. Since $\Delta\mu$ and μ refer to the 1D subchromophore, Equation (8) can directly be compared with the two-level approximation formula [Eq. (9)] used for 1D NLO chromophores. The five-level formula for T -symmetric species actually reduces to a four-level approximation, since the transition from the ground state to the excited A state is symmetry-forbidden.

$$\beta_{ijk}^{2\omega}(\omega) = \frac{1}{6\hbar^2} \sum_{n=1}^m \sum_{n'=1}^m \left[(\mu_{0n}^i \mu_{n'n}^j \mu_{n'n}^k + \mu_{0n}^k \mu_{n'n}^i \mu_{n'n}^j) \left(\frac{1}{(\omega_{0n'} - \omega)(\omega_{0n} + \omega)} + \frac{1}{(\omega_{0n'} + \omega)(\omega_{0n} - \omega)} \right) \right. \\ \left. + (\mu_{0n}^i \mu_{n'n}^j \mu_{n'n}^k + \mu_{0n}^k \mu_{n'n}^i \mu_{n'n}^j) \left(\frac{1}{(\omega_{0n'} + 2\omega)(\omega_{0n} + \omega)} + \frac{1}{(\omega_{0n'} - 2\omega)(\omega_{0n} - \omega)} \right) \right. \\ \left. + (\mu_{0n}^i \mu_{n'n}^k \mu_{n'n}^j + \mu_{0n}^k \mu_{n'n}^i \mu_{n'n}^j) \left(\frac{1}{(\omega_{0n'} - \omega)(\omega_{0n} - 2\omega)} + \frac{1}{(\omega_{0n'} + \omega)(\omega_{0n} + 2\omega)} \right) \right] \quad (7)$$

$$\text{for } \mathbf{3} \quad \beta_{xyz}^{2\omega} = \frac{1}{\hbar^2} \frac{\mu_{02}^x \mu_{22}^y \mu_{22}^z}{\omega_{02}^2} = \frac{1}{\hbar^2} \frac{4}{3\sqrt{3}} \frac{\mu^2 \Delta\mu}{\omega_{02}^2} \quad (8) \quad \beta_{xyz}^{\text{rel}} = 0.770 \mu^2 \Delta\mu$$

$$\text{for } \mathbf{1} \quad \beta_{zzz}^{2\omega} = \frac{1}{\hbar^2} \frac{\mu_{01}^z \mu_{11}^z \mu_{11}^z}{\omega_{01}^2} = \frac{1}{\hbar^2} \frac{\mu^2 \Delta\mu}{\omega_{01}^2} \quad (9) \quad \beta_{zzz}^{\text{rel}} = 1.000 \mu^2 \Delta\mu$$

For **2**, evaluation of Equation (7)^[40] leads to a four-level approximation. Since the transition from the ground state to the A state is allowed, yet weak, there is no simple formula, and Equation (7) has to be evaluated for each β tensor element with the transition moments for the E and A states given above. The results for **2** are given in Equations (10)–(13). Since $\Delta\mu$ of the reference compound **1** is negative, all β_{ijk} values of **2** and **3** are negative, too.

$$-\beta_{yyy}^{\text{rel}} = \beta_{xxx}^{\text{rel}} = 0 \quad (10)$$

$$-\beta_{yyy}^{\text{rel}} = \beta_{xyy}^{\text{rel}} = 0.675 \mu^2 \Delta\mu \quad (11)$$

$$\beta_{yyz}^{\text{rel}} = \beta_{xzx}^{\text{rel}} = 0.364 \mu^2 \Delta\mu \quad (12)$$

$$\beta_{zzz}^{\text{rel}} = 0.053 \mu^2 \Delta\mu \quad (13)$$

F. Theoretical calculations—tensorial approach: Zyss and Oudar^[28, 41] developed mathematical relations between microscopic and macroscopic optical nonlinearities of molecular crystals of a given space group with 1D subunits. It is assumed that the molecules do not interact with each other. We used these relations [Eq. (14)] to deduce the β_{IJK} tensor elements of a molecular chromophore assembly from the β_{ijk} tensor elements of m 1D subchromophores which are related by a given symmetry operation.

$$\beta_{IJK}^{\text{comp}} = \sum_{p=1}^m \sum_{ijk} \cos(\mathbf{I}, \mathbf{i}_p) \cos(\mathbf{J}, \mathbf{j}_p) \cos(\mathbf{K}, \mathbf{k}_p) \beta_{ijk}^{\text{sub}} \quad (14)$$

Here $\beta_{IJK}^{\text{comp}}$ is the tensor element of the composite molecule in the IJK frame and β_{ijk}^{sub} is the tensor element of the submolecule in the molecular ijk frame. In the present case, $\beta_{ijk}^{\text{sub}} = \beta_{zzz}$ of the 1D submolecule **1**. The $\cos(\mathbf{I}, \mathbf{i}_p)$ etc. denote the scalar product of basis vector \mathbf{I} and \mathbf{i} . Detailed expressions for all space groups can be found in ref. [28] and therefore are not given here. The resulting β tensor elements for molecule **2** and **3** can be found in Table 2. The PM3 optimised geometries are used. For compound **3**, the values in D_2 symmetry and in idealised T symmetry are given. The results are identical to those obtained by exciton coupling theory.

Discussion

The UV data presented in Section B suggest that the subchromophores in **2** and **3** are almost electronically independent, since the oscillator strengths behave additively. All compounds show a moderate negative solvatochromism (see Table 1). This can be explained by a change in dipole moment direction upon excitation for **1** and **2** and a change in local charge distribution for **2** and **3** (see Table 2): in polar solvents, the excited Franck–Condon state is placed in a solvent cage with solvent molecules properly oriented to stabilise the ground-state dipole moment. Owing to the wrong solvation sphere, the excited state is destabilised. This destabilisation becomes stronger with increasing solvent polarity; a blue shift results. This discussion also holds true for **3** which, for symmetry reasons, has no dipole moment. However, as **3** has a branched structure, solvent molecules that lie between side arms experience a change in charge distribution and, therefore, local dipole moment of the side arms upon excitation.

As can be seen from Figure 3, negative charge is transferred from the dialkylamino moiety to the phenyl ring adjacent to the phosphonium atom during excitation, and this explains the huge dipole moment difference. The phosphonium group does not act as an electron acceptor; instead it stabilises the negative charge on the phenyl ring by polarisation, similar to ammonium ions.^[6, 42]

Compounds **2** and **3** show absorption maxima slightly red-shifted from that of the 1D chromophore **1**, which can be explained by exciton coupling. For derivative **3**, no Davydov splitting is visible, since the transition to the A state is forbidden; thus, only a red shift of V_{12} is observed; for **2**, the transition to the A state is very weak and hidden under the

broad $A \rightarrow E$ transition. Hence, for **2**, too, no splitting is observed, and the extinction band is also red-shifted. The observed shifts are in good agreement with the dipole–dipole approximation used in exciton coupling theory.

Applying the exciton coupling approach, we also calculated transition moments between the ground state and the excited states, as well as between different excited states. These transition moments were used in the SOS equation [Eq. (7)], which yields β values relative to the 1D subchromophore. For the evaluation of β , we assumed that the transition energies for **1**, **2** and **3** are equal and that the Davydov splitting in **2** and **3** is zero. These assumptions are justified by the small experimentally measured band shifts. Normally, shifts or splittings up to 4000 cm^{-1} are observed in strongly coupling chromophores.^[38a] It becomes clear that although **3** has zero dipole moment, β_{xyz} can be traced back to the dipole moment difference of the subchromophore [see Eq. (8)]. This only holds true for noninteracting or weakly interacting chromophores. For strongly interacting molecules with π overlap, such as 1,3,5-triamino-2,4,6-trinitrobenzene or crystal violet this approach fails. The resulting four-level model for **3** and for **2** involves the same degree of first-order approximation as the traditionally used two-level model for 1D NLO compounds and thus allows direct comparison.

A completely different approach is based on the tensorial properties of β : basis transformation and summation over all β tensor elements of symmetry-related subchromophores also leads to exactly the same relative β_{ijk} values for **1**, **2** and **3**, as does exciton coupling theory. While in the latter approach, the vectorial properties (transition moments) with their phase relations are used, in the former method only the vector component of the β tensor (since we assumed a 1D chromophore) is used. Hence, from a mathematical standpoint it is not surprising that both methods lead to exactly the same results, but from a physical point of view, it is rather startling: the tensorial method simply transforms and adds a given nonlinear optical property of a subchromophore (i.e., the β tensor). In contrast, the exciton coupling method first leads to linear optical properties of the composite molecule (the transition moments) and subsequently, via the perturbation SOS approach, to the second-order nonlinear optical property.

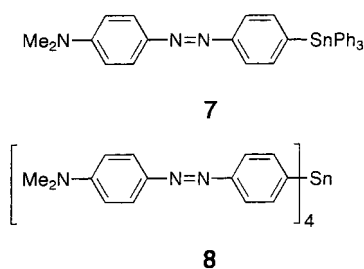
Although **2** has a small dipole moment, the β tensor component along the dipolar z axis is rather small. Therefore, **2** can be viewed as an almost purely octopolar system, like **3**. The TDHF calculations with MOPAC agree very well with the theoretical values for both **2** and for **3** (see Table 2; the numerical agreement of TDHF and experimental absolute results for **1** is fortuitous, since solvent effects were neglected and should lead to smaller calculated values). For **2**, the dipolar component β_{zzz} is almost vanishing. In contrast, the experimental relative β values for **2** and, even more pronounced, for **3** are 32% and 62% higher, respectively, than expected from the theoretical and computational calculations. The red shift of the absorption bands of **2** and **3** relative to **1** due to exciton coupling cannot account for this enhancement, as the shift is much too small. The reason could be that both theoretical methods are based on the assumption that there is only weak interaction between the subchromophores. This is

true as far as the linear optical properties are concerned, as is proved by the good agreement between UV spectra and exciton coupling theory. The TDHF calculations are based on ground-state properties of the molecule; dynamic correlation effects are included within the parametrisation.^[43] Neither the theoretical models nor the TDHF approach includes any further type of correlation effects concerning excited states. However, as can be seen from the four-level model for T symmetric compounds, the transition moment between excited states plays a crucial role and one can expect that nondynamic correlation effects are important in calculating these excited state properties. We suggest that it is the neglect of correlation effects in the theoretical and computational calculations which leads to the underestimation of β in **2** and **3**. This assumption is further supported by semiempirical calculations on triaminotrinitrobenzene at the CISD level, which indicate that electron correlation plays a significant role in describing the first-order nonlinear optical properties of octopolar systems.^[10b, c] In addition, Brouyere et al. found that the AM1/finite-field method underestimates β in calix[4]-arene derivatives due to inadequate inclusion of electron-correlation phenomena.^[44] For our comparative study, in which size consistency is important, this problem could in principle be circumvented by using MP n ab initio calculations or density functional methods and the TDHF approach in order to calculate β on a correlated level. However, the size of the molecules investigated here is beyond our computational capabilities.

Comparison of the modulus of β , derived from experimentally determined $\langle\beta_{\text{HRS}}^2\rangle$ values, reveals that **2**, and to an even greater extent **3**, have considerably higher β values (by a factor of 2.2 to 3.0) than **1** at almost no transparency cost. Comparison of the nonlinear figure of merit, the modulus of β divided by the molecular weight, shows that $||\beta||/M$ increases from the 1D chromophore to the 2D and 3D chromophores: **1**, 0.096; **2**, 0.117; **3**, 0.131.

A series of triarylamine compounds investigated by Stadler et al.^[10f] also have higher β values than the related subchromophores. In this case, however, the composite molecules absorb at distinctly lower energies than the corresponding subunits. The binaphthyl chromophores studied by Wong et al.^[11a] show dipolar coupling enhancement of β only in polar solvents. In both cases, the enhancement was attributed to interchromophoric interactions. Di Bella et al.^[45] investigated in detail the NLO response of p -nitroaniline dimers and trimers in several conformations by INDO/S-SOS calculations. The authors explain the deviation between the calculated β value of the dimers and trimers and the β value derived from an additivity model with the neglect of local-field corrections. This may also account for the subchromophore interactions in **2** and **3**.^[10f]

Compared to the analogous tin compounds **7** ($||\beta^0|| = 57 \times 10^{-30}$ esu in CH_2Cl_2) and **8** ($||\beta^0|| = 116 \times 10^{-30}$ esu in CH_2Cl_2),^[13] the phosphonium derivatives **1**, **2** and **3** have higher β values due to the more efficient phosphonium acceptor; the absorption maxima are also at lower energy (e.g., 20388 cm^{-1} (491 nm) for **1** in CHCl_3 and 23752 cm^{-1} (421 nm) for **7** in CH_2Cl_2). The tetrahedral tin compound **8** also shows an 11% higher β value compared to the 1D tin



compound **7** than theoretically expected. This β exaltation is smaller than in our phosphonium derivatives, but can be explained by the longer Ph–Sn distance (ca. 2.2 Å^[46]) compared to the Ph–P distance (1.82 Å^[16]), which should lead to even weaker subchromophore interactions in the tin compounds than in the phosphonium species.

Conclusions

We have synthesised and investigated two 3D composite NLO chromophores with weakly interacting subchromophore side wings and their 1D reference system. A phosphonium centre was used as the subchromophore connecting unit and as the electron-stabilising (acceptor) group. The β tensor is essentially octopolar in **2** and fully octopolar in **3**. Two independent theoretical approaches (exciton coupling theory and tensor transformation and addition) and one computational method (PM3/TDHF calculations) yield essentially the same relative β_{ijk} values for **1**, **2** and **3**. The experimentally determined values are enhanced for **2** and **3**, probably due to an electron-correlation effect of excited states. The β modulus of **3** is almost three times larger than that of the 1D subchromophore at almost no cost of transparency. This makes octopolar molecules such as **2** and **3** superior with regard to transparency/efficiency trade-off. Optimal nonsymmetric solid-state arrangement of these phosphonium salts could be induced by chiral counterions, for example. This is the topic of further investigations.

Appendix

Eigenvalues E and eigenfunctions ψ for **2** and **3** were obtained from the secular equations [Eqs. (5) and (6)].

We evaluated the transition moments and relative oscillator strengths by using the geometry data of the PM3 optimisation for **2** and by assuming ideal T symmetry for **3**.

Experimental Section

General: All reactions involving n BuLi were carried out in flame-dried Schlenk tubes under nitrogen. THF was dried over sodium/benzophenone ketyl and distilled under nitrogen. The NMR assignments refer to the numbering scheme of **1**.

4-(*N,N*-Dibutylamino)-4'-bromoazobenzene (4-Br) and **4-(*N,N*-dibutylamino)-4'-iodoazobenzene (4-I)** were synthesised by azo coupling reaction from *N,N*-dibutylaniline and 4-bromoaniline in HOAc/NaOAc buffer solution according to ref. [47]. **4-Br:** yield 54%, m.p. 55 °C; C₂₀H₂₆BrN₃ (388.35): calcd C 61.86, H 6.75, N 10.82; found C 61.72, H 6.84, N 10.82. **4-I:** yield 31%, m.p. 53–54 °C; C₂₀H₂₆IN₃ (435.35): calcd C 55.18, H 6.02, N 9.65; found C 55.06, H 5.95, N 9.61.

for **2:**

$$E=E_a+2V_{12} \quad \psi_1 = \frac{1}{\sqrt{3}}\phi_a^{(1)}\phi_0^{(2)}\phi_0^{(3)} + \frac{1}{\sqrt{3}}\phi_0^{(1)}\phi_a^{(2)}\phi_0^{(3)} + \frac{1}{\sqrt{3}}\phi_0^{(1)}\phi_0^{(2)}\phi_a^{(3)}$$

$$E=E_a-V_{12} \quad \psi_2 = \frac{1}{\sqrt{2}}\phi_0^{(1)}\phi_a^{(2)}\phi_0^{(3)} - \frac{1}{\sqrt{2}}\phi_0^{(1)}\phi_0^{(2)}\phi_a^{(3)}$$

$$E=E_a-V_{12} \quad \psi_3 = -\frac{2}{\sqrt{6}}\phi_a^{(1)}\phi_0^{(2)}\phi_0^{(3)} + \frac{1}{\sqrt{6}}\phi_0^{(1)}\phi_a^{(2)}\phi_0^{(3)} + \frac{1}{\sqrt{6}}\phi_0^{(1)}\phi_0^{(2)}\phi_a^{(3)}$$

$$\mu_{01} = \frac{1}{\sqrt{3}}(\mu_{0a}^{(1)} + \mu_{0a}^{(2)} + \mu_{0a}^{(3)}) = (0, 0, 0.4512)\mu \quad f = 0.2036\mu^2$$

$$\mu_{02} = \frac{1}{\sqrt{2}}(\mu_{0a}^{(2)} - \mu_{0a}^{(3)}) = (0, 1.1825, 0)\mu \quad f = 1.3982\mu^2$$

$$\mu_{03} = \frac{1}{\sqrt{6}}(-2\mu_{0a}^{(1)} + \mu_{0a}^{(2)} + \mu_{0a}^{(3)}) = (-1.1825, 0, 0)\mu \quad f = 1.3982\mu^2$$

$$\sum f = 3.0000\mu^2$$

$$\mu_{12} = \frac{1}{\sqrt{6}}(\Delta\mu^{(2)} - \Delta\mu^{(3)}) = (0, 0.6827, 0)\Delta\mu$$

$$\mu_{13} = \frac{1}{3\sqrt{2}}(-2\Delta\mu^{(1)} + \Delta\mu^{(2)} + \Delta\mu^{(3)}) = (-0.6827, 0, 0)\Delta\mu$$

$$\mu_{23} = \frac{1}{2\sqrt{3}}(\Delta\mu^{(2)} - \Delta\mu^{(3)}) = (0, 0.4827, 0)\Delta\mu$$

$$\mu_{11} = \frac{1}{3}(-2\Delta\mu^{(1)} + \Delta\mu^{(2)} + \Delta\mu^{(3)}) = (0, 0, 0.2605)\Delta\mu$$

$$\mu_{22} = \frac{1}{2}(\Delta\mu^{(2)} - \Delta\mu^{(3)}) = (-0.4827, 0, 0.2605)\Delta\mu$$

$$\mu_{33} = \frac{1}{6}(4\Delta\mu^{(1)} + \Delta\mu^{(2)} + \Delta\mu^{(3)}) = (0.4827, 0, 0.2605)\Delta\mu$$

for **3:**

$$E=E_a+3V_{12}$$

$$\psi_1 = \frac{1}{2}(\phi_a^{(1)}\phi_0^{(2)}\phi_0^{(3)}\phi_0^{(4)} + \phi_0^{(1)}\phi_a^{(2)}\phi_0^{(3)}\phi_0^{(4)} + \phi_0^{(1)}\phi_0^{(2)}\phi_a^{(3)}\phi_0^{(4)} + \phi_0^{(1)}\phi_0^{(2)}\phi_0^{(3)}\phi_a^{(4)})$$

$$E=E_a-V_{12}$$

$$\psi_2 = \frac{1}{2}(\phi_a^{(1)}\phi_0^{(2)}\phi_0^{(3)}\phi_0^{(4)} - \phi_0^{(1)}\phi_a^{(2)}\phi_0^{(3)}\phi_0^{(4)} - \phi_0^{(1)}\phi_0^{(2)}\phi_a^{(3)}\phi_0^{(4)} + \phi_0^{(1)}\phi_0^{(2)}\phi_0^{(3)}\phi_a^{(4)})$$

$$E=E_a-V_{12}$$

$$\psi_3 = \frac{1}{2}(\phi_a^{(1)}\phi_0^{(2)}\phi_0^{(3)}\phi_0^{(4)} - \phi_0^{(1)}\phi_a^{(2)}\phi_0^{(3)}\phi_0^{(4)} + \phi_0^{(1)}\phi_0^{(2)}\phi_a^{(3)}\phi_0^{(4)} - \phi_0^{(1)}\phi_0^{(2)}\phi_0^{(3)}\phi_a^{(4)})$$

$$E=E_a-V_{12}$$

$$\psi_4 = \frac{1}{2}(\phi_a^{(1)}\phi_0^{(2)}\phi_0^{(3)}\phi_0^{(4)} + \phi_0^{(1)}\phi_a^{(2)}\phi_0^{(3)}\phi_0^{(4)} - \phi_0^{(1)}\phi_0^{(2)}\phi_a^{(3)}\phi_0^{(4)} - \phi_0^{(1)}\phi_0^{(2)}\phi_0^{(3)}\phi_a^{(4)})$$

$$\mu_{01} = \frac{1}{2}(\mu_{0a}^{(1)} + \mu_{0a}^{(2)} + \mu_{0a}^{(3)} + \mu_{0a}^{(4)}) = 0 \quad f = 0$$

$$\mu_{02} = \frac{1}{2}(\mu_{0a}^{(1)} - \mu_{0a}^{(2)} - \mu_{0a}^{(3)} + \mu_{0a}^{(4)}) = \left(\sqrt{\frac{2}{3}}, -\sqrt{\frac{2}{3}}, 0\right)\mu \quad f = \frac{4}{3}\mu^2$$

$$\mu_{03} = \frac{1}{2}(\mu_{0a}^{(1)} - \mu_{0a}^{(2)} + \mu_{0a}^{(3)} - \mu_{0a}^{(4)}) = \left(-\sqrt{\frac{2}{3}}, -\sqrt{\frac{2}{3}}, 0\right)\mu \quad f = \frac{4}{3}\mu^2$$

$$\mu_{04} = \frac{1}{2}(\mu_{0a}^{(1)} + \mu_{0a}^{(2)} - \mu_{0a}^{(3)} - \mu_{0a}^{(4)}) = \left(0, 0, -\frac{2}{\sqrt{3}}\right)\mu \quad f = \frac{4}{3}\mu^2$$

$$\sum f = 4\mu^2$$

$$\mu_{23} = \frac{1}{4}(\Delta\mu^{(1)} + \Delta\mu^{(2)} - \Delta\mu^{(3)} - \Delta\mu^{(4)}) = \left(0, 0, -\frac{1}{\sqrt{3}}\right)\Delta\mu$$

$$\mu_{24} = \frac{1}{4}(\Delta\mu^{(1)} - \Delta\mu^{(2)} + \Delta\mu^{(3)} - \Delta\mu^{(4)}) = \left(-\frac{1}{\sqrt{6}}, -\frac{1}{\sqrt{6}}, 0\right)\Delta\mu$$

$$\mu_{34} = \frac{1}{4}(\Delta\mu^{(1)} - \Delta\mu^{(2)} - \Delta\mu^{(3)} + \Delta\mu^{(4)}) = \left(\frac{1}{\sqrt{6}}, -\frac{1}{\sqrt{6}}, 0\right)\Delta\mu$$

4-(*N,N*-Dibutylamino)azobenzen-4'-yldiphenylphosphane (5): *n*BuLi (0.81 mL, 1.6 M, 1.3 mmol) in hexanes was added to a solution of 4-Br (388 mg, 1.00 mmol) in THF (5 mL) at -78°C . A dark brown precipitate formed after a few minutes. After 40 min, Ph_2PCl (0.18 mL, 1.00 mmol) was added, and the solution allowed to warm to room temperature. A dark red solution formed and was quenched with a few drops of water; the solvent was removed in vacuo, and the residue purified by column chromatography on silica gel. By-products were eluted first with CH_2Cl_2 /petroleum ether (1/2). The main product was then eluted with CH_2Cl_2 /petroleum ether (1:1). A red oil was obtained (300 mg, 61%), which was air-sensitive and was immediately used for quaternisation. $^1\text{H NMR}$ (250 MHz, CDCl_3): $\delta = 7.83$ (m, 2H, H $2'/6'$), 7.76 (m, 2H, H $3/5'$), 7.36 (2H, H $2/6$), 7.34 (m, 10H, PPh), 6.67 (m, 2H, H $3/5'$), 3.36 (m, 4H, α -H), 1.62 (m, 4H, β -H), 1.38 (m, 4H, γ -H), 0.97 (t, $J = 7.3$ Hz, 6H, δ -H); $^{13}\text{C NMR}$ (62.9 MHz, CDCl_3): $\delta = 153.6$ (C 4), 150.8 (C $1'$), 143.4 (C $4'$), 138.4 (d, $J(\text{C,P}) = 11.7$ Hz, C 1), 137.2 (d, $J(\text{C,P}) = 11.1$ Hz, iC), 134.3 (d, $J(\text{C,P}) = 19.9$ Hz, C $2/6$), 133.8 (d, $J(\text{C,P}) = 19.5$ Hz, o-C), 128.8 (p-C), 128.6 (d, $J(\text{C,P}) = 6.9$ Hz, m-C), 125.4 (C $2'/6'$), 122.1 (d, $J(\text{C,P}) = 7.1$ Hz, C $3/5'$), 111.2 (C $3/5'$), 51.0 (α -C), 29.6 (β -C), 20.3 (γ -C), 13.9 (δ -C).

4-(*N,N*-Dibutylamino)azobenzen-4'-ylmethylidiphenyl-phosphonium iodide (1): MeI (0.3 mL, 4.8 mmol) was added to a solution of 5 (96 mg, 0.19 mmol) in benzene (5 mL). The solution was stirred for 3 h at 40°C . A red oil formed, which solidified while stirring at room temperature for 30 min. The red precipitate was filtered off, washed with benzene and petroleum ether and dried in vacuo (122 mg, 100% of an orange-red powder). M.p. 143°C ; $^1\text{H NMR}$ (400 MHz, CDCl_3): $\delta = 8.02$ (m, 2H, H $3/5'$), 7.86 (m, 2H, H $2'/6'$), 7.84–7.73 (8H, PPh, H $2/6$), 7.73–7.68 (m, 4H, PPh), 6.69 (m, 2H, H $3/5'$), 3.39 (m, 4H, α -H), 3.21 (d, $J = 13.2$ Hz, 3H, PCH_3), 1.64 (m, 4H, β -H), 1.39 (m, 4H, γ -H), 0.98 (t, $J = 7.3$ Hz, 6H, δ -H); $^{13}\text{C NMR}$ (100.6 MHz, CDCl_3): $\delta = 157.4$ (d, $J(\text{C,P}) = 3.3$ Hz, C 4), 151.8 (C $1'$), 143.1 (C $4'$), 135.1 (d, $J(\text{C,P}) = 3.0$ Hz, p-C), 134.2 (d, $J(\text{C,P}) = 11.5$ Hz, C $2/6$), 133.2 (d, $J(\text{C,P}) = 10.8$ Hz, o-C), 130.4 (d, $J(\text{C,P}) = 13.0$ Hz, m-C), 126.5 (C $2'/6'$), 123.5 (d, $J(\text{C,P}) = 13.7$ Hz, C $3/5'$), 119.1 (d, $J(\text{C,P}) = 88.9$ Hz, iC), 117.0 (d, $J(\text{C,P}) = 90.4$ Hz, C 1), 111.1 (C $3/5'$), 51.0 (α -C), 29.4 (β -C), 20.1 (γ -C), 13.8 (δ -C), 11.7 (d, $J(\text{C,P}) = 57.2$ Hz, PCH_3); $\text{C}_{33}\text{H}_{39}\text{IN}_3\text{P} \cdot 0.5\text{H}_2\text{O}$ (644.58): calcd C 61.49, H 6.26, N 6.52; found C 61.45, H 6.46, N 6.48; MS (PI-LSIMS): $m/z = 508$ (K^+); HR-MS (FAB): calcd 508.28816 (K^+), found 508.28985.

Tris[4-(*N,N*-dibutylamino)azobenzen-4'-yl]phosphane (6): *n*BuLi in hexanes (1.89 mL, 1.6 M, 3.0 mmol) was added to a solution of 4-Br (1164 mg, 3.00 mmol) in THF (12 mL) at -78°C . A dark brown precipitate formed after a few minutes. After 40 min PCl_3 (0.079 mL, 0.90 mmol) was added, and the solution stirred for 2.5 h. After further stirring for 45 min at 40°C , a dark red solution formed. The solvent was removed in vacuo, and the residue purified by column chromatography on silica gel under inert gas atmosphere. By-products were eluted first with oxygen-free, nitrogen-saturated CH_2Cl_2 /petroleum ether (1/1); the main product was then eluted with CH_2Cl_2 /petroleum ether (4/1). After removal of the solvent, a red glassy substance was obtained (386 mg, 45%), which was air-sensitive and was immediately used for quaternisation.

Tetrakis[4-(*N,N*-dibutylamino)azobenzen-4'-yl]phosphonium iodide (3): 6 (105 mg, 0.11 mmol), 4-I (48 mg, 0.11 mmol; prepared analogously to 4-Br) and $\text{Pd}(\text{OAc})_2$ (0.4 mg, 0.0018 mmol) were stirred with 1.5 mL of oxygen-free, nitrogen-saturated *p*-xylene under an inert gas atmosphere for 20 h at 140°C . A dark red oil separated. The xylene solution was removed with a pipette and the residue purified by chromatography on silica gel with ethyl acetate/MeOH (10/0.5). A concentrated solution of the product in CH_2Cl_2 was dropped into vigorously stirred petroleum ether. The dark red precipitate was collected by filtration and dried in vacuo. Yield 74 mg (48%). $^1\text{H NMR}$ (250 MHz, CDCl_3): $\delta = 8.09$ (m, 8H, H $3/5'$), 7.90 (m, 8H, H $2'/6'$), 7.75 (m, 8H, H $2/6$), 6.71 (m, 8H, H $3/5'$), 3.41 (m, 16H, α -H), 1.65 (m, 16H, β -H), 1.40 (m, 16H, γ -H), 0.99 (t, $J = 7.2$ Hz, 24H, δ -H); $^{13}\text{C NMR}$ (62.9 MHz, CDCl_3): $\delta = 157.9$ (d, $J(\text{C,P}) = 3.3$ Hz, C 4), 152.3 (C $1'$), 143.5 (C $4'$), 135.4 (d, $J(\text{C,P}) = 11.1$ Hz, C $2/6$), 126.8 (C $2'/6'$), 123.8 (d, $J(\text{C,P}) = 13.7$ Hz, C $3/5'$), 116.2 (d, $J(\text{C,P}) = 92.2$ Hz, C 1), 111.4 (C $3/5'$), 51.1 (α -C), 29.6 (β -C), 20.3 (γ -C), 13.9 (δ -C); $\text{C}_{80}\text{H}_{104}\text{IN}_{12}\text{P} \cdot \text{H}_2\text{O}$ (1409.69): calcd C 68.16, H 7.58, N 11.92; found C 68.17, H 7.58, N 11.66; MS (PI-LSIMS): $m/z = 1263$ (100%, K^+), 1571 (30%, [$\text{K} + \text{dibutylaminoazobenzenyl}$] $^+$); HR-MS (FAB): calcd 1263.82140 (K^+), found 1263.82446.

Tris[4-(*N,N*-dibutylamino)azobenzen-4'-yl]methylphosphonium iodide (2): This compound was directly synthesised from 1.0 mmol 4-Br without isolation of 6 (see above). To the reaction mixture of 6 in THF, MeI (0.8 mL, 13 mmol) was added, and the solution was stirred for 18 h at 40°C in a closed Schlenk tube. The solvent was removed in vacuo, and the residue purified by chromatography on alumina (N, SI) with CH_2Cl_2 /MeOH (10/0.2) and subsequently on silica gel (ethyl acetate/MeOH (10/0.4)). A concentrated solution of the product in ethyl acetate/MeOH was dropped into vigorously stirred petroleum ether. The organic phase was decanted from the resulting dark red oil, which was dried in vacuo to give a glassy substance. Yield 136 mg (41%). $^1\text{H NMR}$ (250 MHz, CDCl_3): $\delta = 8.02$ (m, 6H, H $3/5'$), 7.86 (m, 6H, H $2'/6'$), 7.82 (24H, H $2/6$), 6.69 (m, 6H, H $3/5'$), 3.39 (m, 12H, α -H), 3.25 (d, $J = 13.1$ Hz, 3H, PCH_3), 1.64 (m, 12H, β -H), 1.39 (m, 12H, γ -H), 0.98 (t, $J = 7.3$ Hz, 18H, δ -H); $^{13}\text{C NMR}$ (62.9 MHz, CDCl_3): $\delta = 157.5$ (d, $J(\text{C,P}) = 3.2$ Hz, C 4), 152.0 (C $1'$), 143.4 (C $4'$), 134.3 (d, $J(\text{C,P}) = 11.3$ Hz, C $2/6$), 126.5 (C $2'/6'$), 123.7 (d, $J(\text{C,P}) = 13.8$ Hz, C $3/5'$), 117.8 (d, $J(\text{C,P}) = 90.5$ Hz, C 1), 111.3 (C $3/5'$), 51.1 (α -C), 29.5 (β -C), 20.3 (γ -C), 13.9 (δ -C), 12.3 (d, $J(\text{C,P}) = 69.7$ Hz, PCH_3); $\text{C}_{61}\text{H}_{81}\text{IN}_9\text{P} \cdot 1.5\text{H}_2\text{O}$ (1125.28): calcd C 65.11, H 7.53, N 11.20; found C 65.04, H 7.56, N 10.93; MS(PI-LSIMS): $m/z = 970$ (100%, K^+), 1278 (15%, [$\text{K} + \text{dibutylaminoazobenzenyl}$] $^+$); HR-MS (FAB): calcd 970.63526 (K^+), found 970.63174.

Acknowledgements: This work was supported by the Fonds der Chemischen Industrie (Liebig grant to C.L.), the Deutsche Forschungsgemeinschaft, and the Stiftung Volkswagenwerk. We thank Dr. O. Vostrowsky (Erlangen) for recording the high-resolution mass spectra. C.L. is grateful to Prof. J. Daub for continuous support at Regensburg.

Received: July 2, 1997 [F747]

- [1] For a general introduction to nonlinear optics in organic materials, see a) P. N. Prasad, D. J. Williams, *Nonlinear Optical Effects in Molecules and Polymers*, Wiley, New York, **1991**; b) *Principles and Applications of Nonlinear Optical Materials* (Eds.: R. W. Munn, C. N. Ironside), Blackie, Glasgow, **1993**; c) *Organic Materials for Photonics* (Ed.: G. Zerbi), North Holland, Amsterdam, **1993**; d) T. J. Marks, M. A. Ratner, *Angew. Chem.* **1995**, *107*, 167; *Angew. Chem. Int. Ed. Engl.* **1995**, *34*, 155; e) N. J. Long, *ibid.* **1995**, *107*, 37; **1995**, *34*, 905; f) C. Bosshard, K. Sutter, P. Prêtre, J. Hulliger, M. Flörshömer, P. Kaatz, P. Günther, *Organic Nonlinear Optical Materials*, Gordon and Breach, Basel, **1995**; g) S. R. Marder, J. W. Perry, *Adv. Mater.* **1993**, *5*, 804.
- [2] a) S. R. Marder, D. N. Beratan, L.-T. Cheng, *Science* **1991**, *252*, 103; b) S. R. Marder, C. B. Gorman, B. G. Tiemann, L.-T. Cheng, *J. Am. Chem. Soc.* **1993**, *115*, 3006; c) G. B. Gorman, S. R. Marder, *Proc. Natl. Acad. Sci. USA*, **1993**, *90*, 11297; d) S. R. Marder, L.-T. Cheng, B. G. Tiemann, A. C. Friedli, M. Blanchard-Desce, J. W. Perry, J. Skindhøj, *Science* **1994**, *263*, 511; e) S. R. Marder, C. B. Gorman, F. Meyers, J. W. Perry, G. Bourhill, J.-L. Bredas, B. M. Pierce, *ibid.* **1994**, *265*, 632; f) G. Bourhill, J.-L. Bredas, L.-T. Cheng, S. R. Marder, F. Meyers, J. W. Perry, B. G. Tiemann, *J. Am. Chem. Soc.* **1994**, *116*, 2619; g) F. Meyers, S. R. Marder, B. M. Pierce, J.-L. Bredas, *J. Am. Chem. Soc.* **1994**, *116*, 10703; h) C. Dehu, F. Meyers, E. Hendrickx, K. Clays, A. Persoons, S. R. Marder, J.-L. Bredas, *J. Am. Chem. Soc.* **1995**, *117*, 10127; i) J. D. L. Albert, T. J. Marks, M. A. Ratner, *J. Phys. Chem.* **1996**, *100*, 9714.
- [3] J. L. Oudar, D. S. Chemla, *J. Chem. Phys.* **1977**, *66*, 2664.
- [4] Ref. [1f], Ch. 3.7; L.-T. Cheng, W. Tam, S. H. Stevenson, G. R. Meredith, G. Rikken, S. R. Marder, *J. Phys. Chem.* **1991**, *95*, 10631.
- [5] M. S. Wong, C. Bosshard, F. Pan, P. Günther, *Adv. Mater.* **1996**, *8*, 677.
- [6] a) K. C. Ching, M. Lequan, R.-M. Lequan, A. Grisard, D. Markovitsi, *J. Chem. Soc. Faraday Trans.* **1991**, *87*, 2225; b) C. Lambert, S. Stadler, G. Bourhill, C. Bräuchle, *Angew. Chem.* **1996**, *108*, 710; *Angew. Chem. Int. Ed. Engl.* **1996**, *35*, 644.
- [7] A. Bahl, W. Grahn, S. Stadler, F. Feiner, G. Bourhill, C. Bräuchle, A. Reisner, P. G. Jones, *Angew. Chem.* **1995**, *107*, 1587; *Angew. Chem. Int. Ed. Engl.* **1995**, *34*, 1485.
- [8] a) R. Wortmann, P. Krämer, C. Glania, S. Lebus, N. Detzer, *Chem. Phys.* **1993**, *173*, 99; b) H. S. Nalwa, T. Watanabe, S. Miyata, *Adv. Mater.* **1995**, *7*, 754; c) C. R. Moylan, S. Ermer, S. M. Lovejoy, I.-H. McComb, D. S. Leung, R. Wortmann, P. Krämer, R. J. Twieg, *J. Am.*

- Chem. Soc.* **1996**, *118*, 12950; d) J. J. Wolff, D. Längle, D. Hillenbrand, R. Wortmann, R. Matschiner, C. Glania, P. Krämer, *Adv. Mater.* **1997**, *9*, 138.
- [9] For a review on nonlinear optics in multipolar media, see J. Zyss, I. Ledoux, *Chem. Rev.* **1994**, *94*, 77.
- [10] a) I. Ledoux, J. Zyss, J. S. Siegel, J. Bienne, J.-M. Lehn, *Chem. Phys. Lett.* **1990**, *172*, 440; b) M. Joffre, D. Yaron, R. J. Silbey, J. Zyss, *J. Chem. Phys.* **1992**, *97*, 5607; c) J. L. Bredas, F. Meyers, B. M. Pierce, J. Zyss, *J. Am. Chem. Soc.* **1992**, *114*, 4928; d) J. Zyss, T. C. Van, C. Dhenaut, I. Ledoux, *Chem. Phys.* **1993**, *177*, 281; e) T. Verbiest, K. Clays, C. Samyn, J. Wolff, D. Reinhoudt, A. Persoons, *J. Am. Chem. Soc.* **1994**, *116*, 9320; f) S. Stadler, F. Feiner, C. Bräuchle, S. Brandl, R. Gompper, *Chem. Phys. Lett.* **1995**, *245*, 292; g) Y. Luo, A. Cesar, H. Agren, *ibid.* **1996**, *252*, 389; h) S. Stadler, R. Dietrich, G. Bourhill, C. Bräuchle, *Opt. Lett.* **1996**, *21*, 251.
- [11] a) M. S. Wong, J.-F. Nicoud, C. Runser, A. Fort, M. Barzoukas, E. Marchal, *Chem. Phys. Lett.* **1996**, *253*, 141; b) H.-J. Deussen, E. Hendrickx, C. Boutton, D. Krog, K. Clays, K. Bechgaard, A. Persoons, T. Bjornholm, *J. Am. Chem. Soc.* **1996**, *118*, 6841.
- [12] T. Thami, P. Bassoul, M. A. Petit, J. Simon, A. Fort, M. Barzoukas, A. Villaeys, *J. Am. Chem. Soc.* **1992**, *114*, 915.
- [13] a) M. Lequan, C. Branger, J. Simon, T. Thami, E. Chauchard, A. Persoons, *Chem. Phys. Lett.* **1994**, *229*, 101; b) M. Lequan, C. Branger, J. Simon, T. Thami, E. Chauchard, A. Persoons, *Adv. Mater.* **1994**, *6*, 851.
- [14] See, for example, C. R. Moylan, R. J. Twieg, V. Y. Lee, S. A. Swanson, K. M. Betterton, R. D. Miller, *J. Am. Chem. Soc.* **1993**, *115*, 12599.
- [15] H. Rau, *Angew. Chem.* **1973**, *85*, 248; *Angew. Chem. Int. Ed. Engl.* **1973**, *12*, 224.
- [16] See, for example, A. W. Johnson, *Ylides and Imines of Phosphorus*, Wiley, New York, **1993**.
- [17] a) K. L. Kott, C. M. Whitaker, R. J. McMahon, *Chem. Mater.* **1995**, *7*, 426; b) M. G. Hutchings, P. F. Gordon, P. J. Duggan, I. Ledoux, G. Puccetti, J. Zyss, *Tetrahedron Lett.* **1994**, *35*, 9073.
- [18] T. Migita, T. Nagai, K. Kiuchi, M. Kosugi, *Bull. Chem. Soc. Jpn.* **1983**, *56*, 2869.
- [19] a) K. Clays, A. Persoons, *Phys. Rev. Lett.* **1991**, *66*, 2980; b) K. Clays, A. Persoons, *Rev. Sci. Instrum.* **1992**, *63*, 3285; c) K. Clays, A. Persoons, *Adv. Chem. Phys.* **1993**, *3*, 456.
- [20] S. Stadler, R. Dietrich, G. Bourhill, C. Bräuchle, A. Pawlik, W. Grahn, *Chem. Phys. Lett.* **1995**, *247*, 271.
- [21] S. Stadler, G. Bourhill, C. Bräuchle, *J. Phys. Chem.* **1996**, *100*, 6927.
- [22] Although polarised HRS measurements would give more information about the β tensor elements, only unpolarised detection of the HRS signal was applicable in the present case for two reasons: 1) The photomultiplier sensitivity at the second harmonic frequency (650 nm) is rather low and polarisation would further weaken the HRS signal. 2) We use an essentially collimated laser beam in a tubular HRS cell (see ref. [20]). The HRS signal is detected perpendicular to the tube axis over a length of ca. 5 cm without additional focusing optics. This set-up does not allow polarised detection (see ref. [23]).
- [23] a) P. Kaatz, D. P. Shelton, *J. Chem. Phys.* **1996**, *105*, 3918; b) I. D. Morrison, R. G. Dunning, W. M. Laidlaw, M. A. Stammers, *Rev. Sci. Instrum.* **1996**, *67*, 1445.
- [24] M. Stähelin, D. M. Burland, J. E. Rice, *Chem. Phys. Lett.* **1992**, *191*, 245.
- [25] A. Willetts, J. E. Rice, D. M. Burland, D. P. Shelton, *J. Chem. Phys.* **1992**, *97*, 7590.
- [26] F. Feiner, Ph.D. Thesis, Ludwig-Maximilians-Universität München, **1995**.
- [27] a) S. J. Cyvin, J. E. Rauch, J. C. Decius, *J. Chem. Phys.* **1965**, *43*, 4083; b) R. Behrson, Y.-H. Pao, H. L. Frisch, *J. Chem. Phys.* **1966**, *45*, 3184.
- [28] a) J. L. Oudar, J. Zyss, *Phys. Rev. A.* **1982**, *26*, 2016; b) J. Zyss, J. L. Oudar, *Phys. Rev. A.* **1982**, *26*, 2028.
- [29] MOPAC 93, Fujitsu, Japan 1993.
- [30] J. Fabian, H. Hauptmann, *Light Absorption of Organic Colorants*, Springer, Berlin, **1980**, p. 46, and references therein.
- [31] The dipole moment of charged species is not well-defined and is origin-dependent. The MOPAC program uses a mass-centred origin for the calculation of dipole moments. However, the dipole moment differences of different states are observable quantities: see D. Buckingham, *Quart. Rev.* **1959**, *13*, 183.
- [32] A. Klamt, G. Schüürmann, *J. Chem. Soc. Perkin Trans. 2*, **1993**, 799.
- [33] S. P. Karna, M. Dupuis, *J. Comput. Chem.* **1991**, *12*, 487.
- [34] For a review on quantum-chemical calculations of NLO properties of organic and organometallic compounds, see D. R. Kanis, M. A. Ratner, T. J. Marks, *Chem. Rev.* **1994**, *94*, 195.
- [35] Using the SOS formalism based on CI expansions, one encounters several problems when comparing β values of molecules of different size. While CIS calculations are size-consistent with respect to the ground-state energy, they only include a small portion of electron correlation for the excited states due to singles–singles coupling. Although INDO/S is parametrised at the CIS level to reproduce first excited state energies, higher excited states which are important (although to a lesser extent than the first excited state) for the SOS formalism are not included in the parametrisation. In contrast, CISD expansions include electron correlation both for the ground state and for the excited states and should therefore allow more accurate calculations of higher excited-state properties, especially when electron correlation of excited states is expected to be very important, as in our case. However, CISD expansions are not size-consistent, and there seems to be no way to guarantee the same degree of electron correlation of ground and excited states for systems of different size. In addition, the SOS expansions tend to converge much more slowly for CISD calculations than for CIS calculations. Although we have tried to study the NLO response of **1–3** by INDO/S-CIS-SOS and PM3/PECI-SOS^[36] methods, consistent and converged values were not obtained, and they are therefore omitted here.^[37]
- [36] T. Clark, J. Chandrasekhar, *Israel. J. Chem.* **1993**, *33*, 435.
- [37] For a discussion of correlation effects on nonlinear optical properties, see a) I. D. L. Albert, T. J. Marks, M. A. Ratner in *Nonlinear Optical Materials* (Eds.: S. P. Karna, A. T. Yeates), *ACS Symp. Ser.* 628, ACS, Washington, **1996**, p. 116; b) P. N. Prasad, S. P. Karna, *Int. J. Quantum. Chem.* **1994**, *S28*, 395.
- [38] a) E. G. McRae, M. Kasha, in *Physical Processes in Radiation Biology* (Eds.: L. Augenstein, R. Mason, B. Rosenberg), Academic Press, New York, **1964**, p. 23; b) M. Kasha, H. R. Rawls, M. Asharf El-Bayoumi, *Pure Appl. Chem.* **1965**, *11*, 371; c) N. Harada, K. Nakanishi, *Circular Dichroic Spectroscopy—Exciton Coupling in Organic Stereochemistry*, Oxford University Press, Oxford, **1983**, Ch. X.
- [39] The PM3 calculated ΔH , for the reaction **31** \rightarrow **2** + 2[P(CH₃)Ph₃]⁺ is 0.84 kJ mol⁻¹.
- [40] V. J. Docherty, D. Pugh, J. O. Morley, *J. Chem. Soc. Faraday Trans. 2*, **1985**, *81*, 1179. The centre of charge has been used as the origin, which then gives $\mu_{00} = 0$. This has no physical meaning and leads only to a mathematical simplification, as only dipole moment differences enter Equations (8) and (9) (see ref. [31]).
- [41] See also ref. [24]; B. Dick, *Chem. Phys.* **1985**, *96*, 199.
- [42] For a discussion of the anion-stabilising effect of phosphonium groups, see ref. [16], Ch. 2.4.
- [43] T. Clark in *Recent Experimental and Computational Advances in Molecular Spectroscopy* (Ed.: R. Fausto), Kluwer Academic, **1993**, p. 369.
- [44] E. Brouyere, A. Persoons, J. L. Bredas, *J. Phys. Chem. A* **1997**, *101*, 4142.
- [45] S. Di Bella, M. A. Rantner, T. J. Marks, *J. Am. Chem. Soc.* **1992**, *114*, 5842.
- [46] *CRC Handbook of Chemistry and Physics, 1st Student Ed.* (Ed.: R. C. Weast), CRC, Boca Raton, Florida, **1988**, p. F106.
- [47] *Organikum*, VEB Deutscher Verlag der Wissenschaften, **1986**, p. 549.